

Improved measurement of $\overline{B}^0 \rightarrow D_s^- D^+$ and
 search for $\overline{B}^0 \rightarrow D_s^+ D_s^-$ at Belle

K. Abe,⁹ K. Abe,⁴⁷ I. Adachi,⁹ H. Aihara,⁴⁹ K. Aoki,²³ K. Arinstein,² Y. Asano,⁵⁴
 T. Aso,⁵³ V. Aulchenko,² T. Aushev,¹³ T. Aziz,⁴⁵ S. Bahinipati,⁵ A. M. Bakich,⁴⁴
 V. Balagura,¹³ Y. Ban,³⁶ S. Banerjee,⁴⁵ E. Barberio,²² M. Barbero,⁸ A. Bay,¹⁹ I. Bedny,²
 U. Bitenc,¹⁴ I. Bizjak,¹⁴ S. Blyth,²⁵ A. Bondar,² A. Bozek,²⁹ M. Bračko,^{9,21,14}
 J. Brodzicka,²⁹ T. E. Browder,⁸ M.-C. Chang,⁴⁸ P. Chang,²⁸ Y. Chao,²⁸ A. Chen,²⁵
 K.-F. Chen,²⁸ W. T. Chen,²⁵ B. G. Cheon,⁴ C.-C. Chiang,²⁸ R. Chistov,¹³ S.-K. Choi,⁷
 Y. Choi,⁴³ Y. K. Choi,⁴³ A. Chuvikov,³⁷ S. Cole,⁴⁴ J. Dalseno,²² M. Danilov,¹³ M. Dash,⁵⁶
 L. Y. Dong,¹¹ R. Dowd,²² J. Dragic,⁹ A. Drutskoy,⁵ S. Eidelman,² Y. Enari,²³ D. Epifanov,²
 F. Fang,⁸ S. Fratina,¹⁴ H. Fujii,⁹ N. Gabyshev,² A. Garmash,³⁷ T. Gershon,⁹ A. Go,²⁵
 G. Gokhroo,⁴⁵ P. Goldenzweig,⁵ B. Golob,^{20,14} A. Gorišek,¹⁴ M. Grosse Perdekamp,³⁸
 H. Guler,⁸ R. Guo,²⁶ J. Haba,⁹ K. Hara,⁹ T. Hara,³⁴ Y. Hasegawa,⁴² N. C. Hastings,⁴⁹
 K. Hasuko,³⁸ K. Hayasaka,²³ H. Hayashii,²⁴ M. Hazumi,⁹ T. Higuchi,⁹ L. Hinz,¹⁹ T. Hojo,³⁴
 T. Hokuue,²³ Y. Hoshi,⁴⁷ K. Hoshina,⁵² S. Hou,²⁵ W.-S. Hou,²⁸ Y. B. Hsiung,²⁸
 Y. Igarashi,⁹ T. Iijima,²³ K. Ikado,²³ A. Imoto,²⁴ K. Inami,²³ A. Ishikawa,⁹ H. Ishino,⁵⁰
 K. Itoh,⁴⁹ R. Itoh,⁹ M. Iwasaki,⁴⁹ Y. Iwasaki,⁹ C. Jacoby,¹⁹ C.-M. Jen,²⁸ R. Kagan,¹³
 H. Kakuno,⁴⁹ J. H. Kang,⁵⁷ J. S. Kang,¹⁶ P. Kapusta,²⁹ S. U. Kataoka,²⁴ N. Katayama,⁹
 H. Kawai,³ N. Kawamura,¹ T. Kawasaki,³¹ S. Kazi,⁵ N. Kent,⁸ H. R. Khan,⁵⁰
 A. Kibayashi,⁵⁰ H. Kichimi,⁹ H. J. Kim,¹⁸ H. O. Kim,⁴³ J. H. Kim,⁴³ S. K. Kim,⁴¹
 S. M. Kim,⁴³ T. H. Kim,⁵⁷ K. Kinoshita,⁵ N. Kishimoto,²³ S. Korpar,^{21,14} Y. Kozakai,²³
 P. Krizan,^{20,14} P. Krokovny,⁹ T. Kubota,²³ R. Kulasiri,⁵ C. C. Kuo,²⁵ H. Kurashiro,⁵⁰
 E. Kurihara,³ A. Kusaka,⁴⁹ A. Kuzmin,² Y.-J. Kwon,⁵⁷ J. S. Lange,⁶ G. Leder,¹²
 S. E. Lee,⁴¹ Y.-J. Lee,²⁸ T. Lesiak,²⁹ J. Li,⁴⁰ A. Limosani,⁹ S.-W. Lin,²⁸ D. Liventsev,¹³
 J. MacNaughton,¹² G. Majumder,⁴⁵ F. Mandl,¹² D. Marlow,³⁷ H. Matsumoto,³¹
 T. Matsumoto,⁵¹ A. Matyja,²⁹ Y. Mikami,⁴⁸ W. Mitaroff,¹² K. Miyabayashi,²⁴ H. Miyake,³⁴
 H. Miyata,³¹ Y. Miyazaki,²³ R. Mizuk,¹³ D. Mohapatra,⁵⁶ G. R. Moloney,²² T. Mori,⁵⁰
 A. Murakami,³⁹ T. Nagamine,⁴⁸ Y. Nagasaka,¹⁰ T. Nakagawa,⁵¹ I. Nakamura,⁹
 E. Nakano,³³ M. Nakao,⁹ H. Nakazawa,⁹ Z. Natkaniec,²⁹ K. Neichi,⁴⁷ S. Nishida,⁹
 O. Nitoh,⁵² S. Noguchi,²⁴ T. Nozaki,⁹ A. Ogawa,³⁸ S. Ogawa,⁴⁶ T. Ohshima,²³ T. Okabe,²³
 S. Okuno,¹⁵ S. L. Olsen,⁸ Y. Onuki,³¹ W. Ostrowicz,²⁹ H. Ozaki,⁹ P. Pakhlov,¹³ H. Palka,²⁹
 C. W. Park,⁴³ H. Park,¹⁸ K. S. Park,⁴³ N. Parslow,⁴⁴ L. S. Peak,⁴⁴ M. Pernicka,¹²
 R. Pestotnik,¹⁴ M. Peters,⁸ L. E. Piilonen,⁵⁶ A. Poluektov,² F. J. Ronga,⁹ N. Root,²
 M. Rozanska,²⁹ H. Sahoo,⁸ M. Saigo,⁴⁸ S. Saitoh,⁹ Y. Sakai,⁹ H. Sakamoto,¹⁷
 H. Sakaue,³³ T. R. Sarangi,⁹ M. Satapathy,⁵⁵ N. Sato,²³ N. Satoyama,⁴² T. Schietinger,¹⁹
 O. Schneider,¹⁹ P. Schönmeier,⁴⁸ J. Schümann,²⁸ C. Schwanda,¹² A. J. Schwartz,⁵
 T. Seki,⁵¹ K. Senyo,²³ R. Seuster,⁸ M. E. Sevier,²² T. Shibata,³¹ H. Shibuya,⁴⁶ J.-G. Shiu,²⁸
 B. Shwartz,² V. Sidorov,² J. B. Singh,³⁵ A. Somov,⁵ N. Soni,³⁵ R. Stamen,⁹ S. Stanič,³²
 M. Starič,¹⁴ A. Sugiyama,³⁹ K. Sumisawa,⁹ T. Sumiyoshi,⁵¹ S. Suzuki,³⁹ S. Y. Suzuki,⁹
 O. Tajima,⁹ N. Takada,⁴² F. Takasaki,⁹ K. Tamai,⁹ N. Tamura,³¹ K. Tanabe,⁴⁹
 M. Tanaka,⁹ G. N. Taylor,²² Y. Teramoto,³³ X. C. Tian,³⁶ K. Trabelsi,⁸ Y. F. Tse,²²

T. Tsuboyama,⁹ T. Tsukamoto,⁹ K. Uchida,⁸ Y. Uchida,⁹ S. Uehara,⁹ T. Uglov,¹³
 K. Ueno,²⁸ Y. Unno,⁹ S. Uno,⁹ P. Urquijo,²² Y. Ushiroda,⁹ G. Varner,⁸ K. E. Varvell,⁴⁴
 S. Villa,¹⁹ C. C. Wang,²⁸ C. H. Wang,²⁷ M.-Z. Wang,²⁸ M. Watanabe,³¹ Y. Watanabe,⁵⁰
 L. Widhalm,¹² C.-H. Wu,²⁸ Q. L. Xie,¹¹ B. D. Yabsley,⁵⁶ A. Yamaguchi,⁴⁸ H. Yamamoto,⁴⁸
 S. Yamamoto,⁵¹ Y. Yamashita,³⁰ M. Yamauchi,⁹ Heyoung Yang,⁴¹ J. Ying,³⁶
 S. Yoshino,²³ Y. Yuan,¹¹ Y. Yusa,⁴⁸ H. Yuta,¹ S. L. Zang,¹¹ C. C. Zhang,¹¹ J. Zhang,⁹
 L. M. Zhang,⁴⁰ Z. P. Zhang,⁴⁰ V. Zhilich,² T. Ziegler,³⁷ A. Zupanc,¹⁴ and D. Zürcher¹⁹

(The Belle Collaboration)

¹*Aomori University, Aomori*

²*Budker Institute of Nuclear Physics, Novosibirsk*

³*Chiba University, Chiba*

⁴*Chonnam National University, Kwangju*

⁵*University of Cincinnati, Cincinnati, Ohio 45221*

⁶*University of Frankfurt, Frankfurt*

⁷*Gyeongsang National University, Chinju*

⁸*University of Hawaii, Honolulu, Hawaii 96822*

⁹*High Energy Accelerator Research Organization (KEK), Tsukuba*

¹⁰*Hiroshima Institute of Technology, Hiroshima*

¹¹*Institute of High Energy Physics,*

Chinese Academy of Sciences, Beijing

¹²*Institute of High Energy Physics, Vienna*

¹³*Institute for Theoretical and Experimental Physics, Moscow*

¹⁴*J. Stefan Institute, Ljubljana*

¹⁵*Kanagawa University, Yokohama*

¹⁶*Korea University, Seoul*

¹⁷*Kyoto University, Kyoto*

¹⁸*Kyungpook National University, Taegu*

¹⁹*Swiss Federal Institute of Technology of Lausanne, EPFL, Lausanne*

²⁰*University of Ljubljana, Ljubljana*

²¹*University of Maribor, Maribor*

²²*University of Melbourne, Victoria*

²³*Nagoya University, Nagoya*

²⁴*Nara Women's University, Nara*

²⁵*National Central University, Chung-li*

²⁶*National Kaohsiung Normal University, Kaohsiung*

²⁷*National United University, Miao Li*

²⁸*Department of Physics, National Taiwan University, Taipei*

²⁹*H. Niewodniczanski Institute of Nuclear Physics, Krakow*

³⁰*Nippon Dental University, Niigata*

³¹*Niigata University, Niigata*

³²*Nova Gorica Polytechnic, Nova Gorica*

³³*Osaka City University, Osaka*

³⁴*Osaka University, Osaka*

³⁵*Panjab University, Chandigarh*

³⁶*Peking University, Beijing*

³⁷*Princeton University, Princeton, New Jersey 08544*

³⁸*RIKEN BNL Research Center, Upton, New York 11973*

³⁹*Saga University, Saga*

⁴⁰*University of Science and Technology of China, Hefei*

⁴¹*Seoul National University, Seoul*

⁴²*Shinshu University, Nagano*

⁴³*Sungkyunkwan University, Suwon*

⁴⁴*University of Sydney, Sydney NSW*

⁴⁵*Tata Institute of Fundamental Research, Bombay*

⁴⁶*Toho University, Funabashi*

⁴⁷*Tohoku Gakuin University, Tagajo*

⁴⁸*Tohoku University, Sendai*

⁴⁹*Department of Physics, University of Tokyo, Tokyo*

⁵⁰*Tokyo Institute of Technology, Tokyo*

⁵¹*Tokyo Metropolitan University, Tokyo*

⁵²*Tokyo University of Agriculture and Technology, Tokyo*

⁵³*Toyama National College of Maritime Technology, Toyama*

⁵⁴*University of Tsukuba, Tsukuba*

⁵⁵*Utkal University, Bhubaneswer*

⁵⁶*Virginia Polytechnic Institute and State University, Blacksburg, Virginia 24061*

⁵⁷*Yonsei University, Seoul*

Abstract

We reconstruct $\bar{B}^0 \rightarrow D_s^- D^+$ decays using a sample of 275×10^6 $B\bar{B}$ pairs recorded by the Belle experiment, and we measure the branching fraction to be $[7.42 \pm 0.23(\text{stat.}) \pm 1.36(\text{syst.})] \times 10^{-3}$. We also search for the related decay $\bar{B}^0 \rightarrow D_s^+ D_s^-$. We observe no statistically significant signal and set an upper limit on the branching fraction of 2.0×10^{-4} at 90% C.L.

PACS numbers: 13.25.Hw, 14.40.Nd

Introduction

Several decay modes of B mesons with D_s^+ in the final state have been measured at the B factories. The amplitudes governing these decays are interesting because neither constituent flavor of the D_s^+ is present in the initial state. For example, the recently-observed decays $\bar{B}^0 \rightarrow D_s^+ K^-$ [1] and $\bar{B}^0 \rightarrow D_{sJ}^+(2317) K^-$ [2], with branching fractions in the range $10^{-5} - 10^{-4}$, can proceed via a $b\bar{d} \rightarrow c\bar{u}$ W -exchange diagram. Here we study the related decays $\bar{B}^0 \rightarrow D_s^+ D_s^-$ and $\bar{B}^0 \rightarrow D_s^- D^+$. The former proceeds via Cabibbo-suppressed W -exchange and has not yet been observed; a recent theoretical calculation predicts a branching fraction of $\sim 2.5 \times 10^{-4}$ [3]. The latter proceeds via a Cabibbo-favored tree diagram; the ratio of its branching fraction to that for $\bar{B}^0 \rightarrow D_s^+ \pi^-$ can be used to determine the ratio of CKM matrix elements $|V_{ub}/V_{cb}|$ [4] assuming factorization [5]. However, the PDG value [6] for $B(\bar{B}^0 \rightarrow D_s^+ D^-)$ has a large uncertainty (38%), which limits the usefulness of this method at present.

In this paper we report an improved measurement of $\bar{B}^0 \rightarrow D_s^- D^+$ decays and a search for $\bar{B}^0 \rightarrow D_s^+ D_s^-$ decays with the Belle detector [7] at the KEKB asymmetric energy e^+e^- collider [8]. The results are based on a 253 fb^{-1} data sample collected at the center-of-mass (CM) energy of the $\Upsilon(4S)$ resonance. To study backgrounds, we used a Monte Carlo (MC) simulated sample of $\Upsilon(4S) \rightarrow B\bar{B}$ events and $e^+e^- \rightarrow q\bar{q}$ ($q = u, d, s$ and c quarks) continuum events; the sample size was about twice that of the data. To evaluate the reconstruction efficiency, we used a large MC sample of several thousand signal events.

The Belle detector is a large-solid-angle magnetic spectrometer that consists of a multi-layer silicon vertex detector (SVD), a 50-layer central drift chamber (CDC), an array of aerogel threshold Čerenkov counters (ACC), a barrel-like arrangement of time-of-flight scintillation counters (TOF), and an electromagnetic calorimeter (ECL) comprised of CsI(Tl) crystals located inside a superconducting solenoid coil that provides a 1.5 T magnetic field. An iron flux-return located outside of the coil is instrumented to detect K_L^0 mesons and to identify muons (KLM). The detector is described in detail elsewhere [7]. Two different inner detector configurations were used. For the first 152 million $B\bar{B}$ pairs, a 2.0 cm radius beampipe and a 3-layer silicon vertex detector were used; for the latter 123 million $B\bar{B}$ pairs, a 1.5 cm radius beampipe, a 4-layer silicon detector and a small-cell inner drift chamber were used [10].

Charged tracks were selected with loose requirements on the impact parameter relative to the interaction point (IP). We also required the transverse momentum of the tracks to be greater than 0.2 GeV/ c in order to reduce low momentum combinatorial background. Based on the optimization of the product of the efficiency and sample purity as evaluated by MC, we impose the following requirements. For charged particle identification (PID) we combined information from the CDC, TOF and ACC counters into a likelihood ratio $\mathcal{L}(K^\pm)/(\mathcal{L}(K^\pm) + \mathcal{L}(\pi^\pm))$ [11], which we required to be larger(smaller) than 0.5 for charged kaon(pion) candidates. This requirement selected kaons and pions with average efficiencies of 92% and 96%, respectively. Neutral kaons (K_S^0) were reconstructed using pairs of oppositely-charged tracks that have an invariant mass within 30 MeV/ c^2 of the nominal K^0 mass, and a displaced vertex from the IP. We used the $D_s^- \rightarrow \phi\pi^-$, $K^{*0}K^-$, and $K_S^0K^-$ modes to reconstruct D_s^- mesons and $D^+ \rightarrow K^+K^-\pi^+$, $K^-\pi^+\pi^+$, and $K_S^0\pi^+$ for the D^+ mesons [12]. Combinations of oppositely-charged kaons with $|M_\phi - M_{K^+K^-}| < 20 \text{ MeV}/c^2$ and of oppositely-charged kaons and pions with $|M_{K^{*0}} - M_{K^+\pi^-}| < 85 \text{ MeV}/c^2$ were retained as ϕ and K^{*0} candidates, respectively, where M_ϕ and $M_{K^{*0}}$ are the nominal masses of the

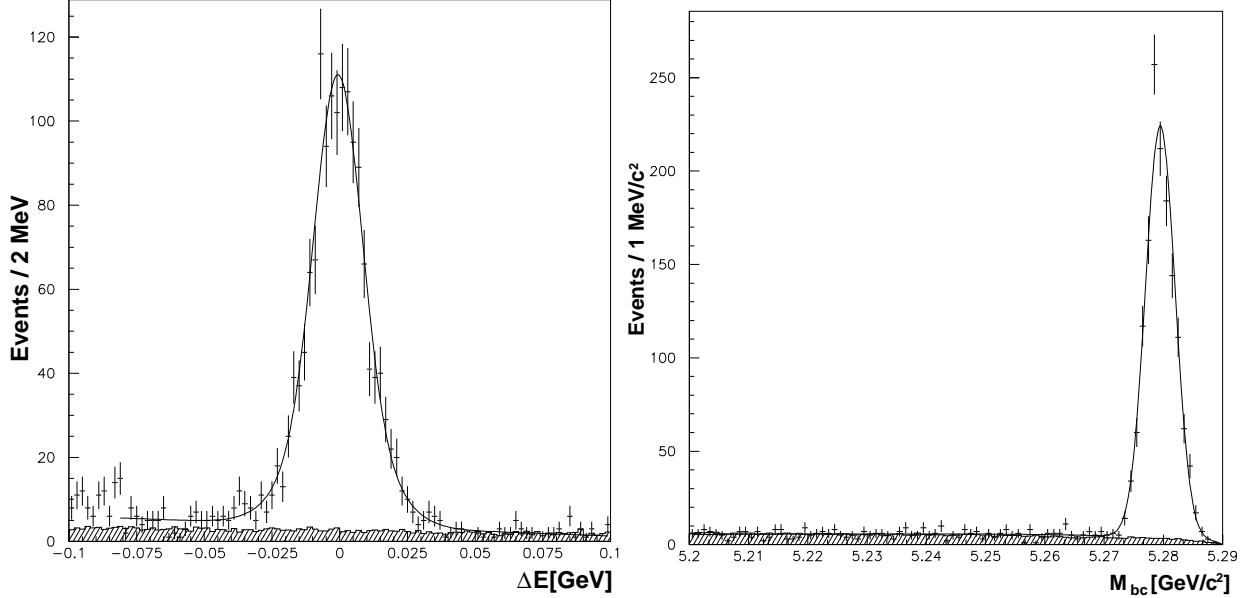


FIG. 1: ΔE (left) and M_{bc} (right) distributions for reconstructed $\overline{B}^0 \rightarrow D_s^- D^+$ events in the M_{bc} or ΔE signal region, respectively. The curve shows the results of the fit. The normalized distributions for the events in the sideband of D_s and D meson masses are shown as the hatched histograms.

two mesons [6]. These combinations, as well as K_S^0 's, were then combined with a K^\pm or π^\pm to form D_s^\pm mesons. All combinations with invariant masses within a 4σ (4.5σ) interval around the nominal D_s^\pm (D^\pm) mass were considered for further analysis. The values of σ were determined from invariant mass distributions of MC D_s^\pm (D^\pm) decays and were in the range $3.6 - 4.2 \text{ MeV}/c^2$.

Pairs of D_s^- and $D_{(s)}^+$ meson candidates were combined to form \overline{B}^0 meson candidates. These were identified by their CM energy difference, $\Delta E = E_B^{\text{CM}} - E_{\text{beam}}^{\text{CM}}$, and the beam constrained mass, $M_{bc} = \sqrt{(E_{\text{beam}}^{\text{CM}})^2 - (p_B^{\text{CM}})^2}$, where $E_{\text{beam}}^{\text{CM}} = \sqrt{s}/2$ is the CM beam energy and E_B^{CM} and p_B^{CM} are the reconstructed energy and momentum of the B meson candidate in the CM frame. We retained events having $M_{bc} > 5.2 \text{ GeV}/c^2$ and $|\Delta E| < 0.2 \text{ GeV}$. The signal region was defined as $5.272 \text{ GeV}/c^2 \leq M_{bc} \leq 5.285 \text{ GeV}/c^2$ and $|\Delta E| \leq 0.025 \text{ GeV}$.

To suppress the large combinatorial background dominated by the two-jet-like $e^+e^- \rightarrow q\bar{q}$ continuum process, variables characterizing the event topology were used. We required the ratio of the second to zeroth Fox-Wolfram moments [13] $R_2 < 0.3$ and the thrust value of the event $T < 0.8$. Simulation showed that this selection retained more than 95% of $B\bar{B}$ events and rejected about 55% of $c\bar{c}$ events and 65% of $u\bar{u}$, $d\bar{d}$ and $s\bar{s}$ events.

$\overline{B}^0 \rightarrow D_s^- D^+$ decays

The ΔE and M_{bc} distributions for $\overline{B}^0 \rightarrow D_s^- D^+$ decays obtained after applying all selection criteria described above are shown in Fig. 1.

The beam-constrained mass distribution is well-described using a Gaussian function for the signal and an empirically parameterized background shape introduced by the ARGUS

Collaboration [14]. The energy difference is described using two Gaussians with the same mean for the signal and a linear function for the background. The normalizations, positions and widths of the signal are free parameters of the binned likelihood fit. The solid lines in Fig. 1 show the result of fits in the interval $-0.08 \text{ GeV} < \Delta E < 0.10 \text{ GeV}$ and $5.20 \text{ GeV}/c^2 < M_{bc} < 5.29 \text{ GeV}/c^2$. The fit to the ΔE distribution for events in the M_{bc} signal region gives a signal yield of $N_{\text{data}} = 1372 \pm 42$ events. The width of the narrower Gaussian that contains about 66% of the signal is $8.6 \pm 0.9 \text{ MeV}$. From the fit to the M_{bc} distribution for events in the ΔE signal region we find 1381 ± 45 signal events. Due to the simpler parameterization of the energy difference distribution and possible peaking background in the M_{bc} distribution, we choose to evaluate all the results from the fits to the ΔE distribution for events within the M_{bc} signal region. While the level of the combinatorial background is found to be low, we used events in the sidebands of the D_s and D meson invariant mass distributions to check for possible remaining peaking background as described later.

The efficiency of the selection criteria depends weakly on the reconstructed decay channel of the charmed mesons. Efficiencies as obtained from the simulated event sample for different combinations of D and D_s meson decay channels are used for calculation of the overall efficiency. The efficiency includes intermediate branching fractions: $\epsilon(D_s D) = \sum_{i,j=1,3} \epsilon_{i,j} \mathcal{B}(D_{si}) \mathcal{B}(D_j) = (6.31 \pm 0.88) \times 10^{-4}$. Here, $\epsilon_{i,j}$ represents the efficiency for reconstructing the event if the D_s meson decays through the i -th mode and the D meson through the j -th mode. The largest part of the uncertainty ($\pm 13.9\%$) arises due to the uncertainties in the intermediate branching fractions [6, 15]. There is also a small contribution due to limited MC statistics. Alternatively, one can express the efficiency in terms of that for $\mathcal{B}(D_s^+ \rightarrow \phi\pi^+)$, relative to which the branching fractions for $D_s^- \rightarrow K^{*0}K^-$ and $D_s^- \rightarrow K_S^0 K^-$ are well-measured [6]. In this case we obtain $\epsilon(D_s D) = (3.18 \pm 0.25) \times 10^{-2} \cdot \mathcal{B}(D_s^+ \rightarrow \phi\pi^+) \mathcal{B}(\phi \rightarrow K^+ K^-)$.

The signal peak includes non-resonant $D_s^- \rightarrow K^+ K^- \pi^-$ decays resulting in the same final state. By fitting the ΔE distributions of a simulated sample we evaluate the fraction of such decays with respect to reconstructed $\overline{B}^0 \rightarrow D_s^- D^+$ decays to be $r_{KK\pi} = (3.46 \pm 0.74)\%$. For the final evaluation of the systematic error we include the uncertainty on the branching fraction for the non-resonant $D_s^- \rightarrow K^+ K^- \pi^-$ decays [6]. This increases the error on $r_{KK\pi}$, which becomes $(3.46 \pm 1.70)\%$. Due to their small contribution to the signal, the nonresonant component is not included in the branching fraction calculation.

The ΔE and M_{bc} distributions obtained using events in the sidebands of both the D and D_s mesons are in agreement with the observed background under the $\overline{B}^0 \rightarrow D_s^- D^+$ signal. No peaking is observed for events in the D mass sideband; however, peaking is observed in the D_s mass sideband as shown in Fig. 2. A peaking component in the $D_s^- \rightarrow K^{*0}K^-$ decay mode is due to the three-body decay $\overline{B}^0 \rightarrow D^+ K^{*0}K^-$, previously reported by Belle [16]. Since the $K^{*0}K^-$ invariant mass in these decays also populates the region under the D_s^- peak, we must subtract this contribution from the signal. By fitting the ΔE distribution of the D_s sideband and normalizing the yield to the area under the D_s peak, we determine the fraction of such three-body decays within the $\overline{B}^0 \rightarrow D_s^- D^+$ signal peak to be $r_{DK^*K} = (2.74 \pm 0.57)\%$. Since the method assumes approximately equal contributions of $\overline{B}^0 \rightarrow D^+ K^{*0}K^-$ decays in the D_s sidebands and in the signal region, we assign an additional systematic error to r_{DK^*K} . From the $K^{*0}K^-$ invariant mass distribution given in [16], we estimate a possible relative change in the yield over the relevant $M(K^{*0}K^-)$ interval ($1.77 \text{ GeV}/c^2 \leq M(K^{*0}K^-) \leq 2.17 \text{ GeV}/c^2$) to be $\pm 40\%$. With the inclusion of this additional uncertainty, the fraction r_{DK^*K} is $(2.74 \pm 1.24)\%$. The signal peak in Fig. 2

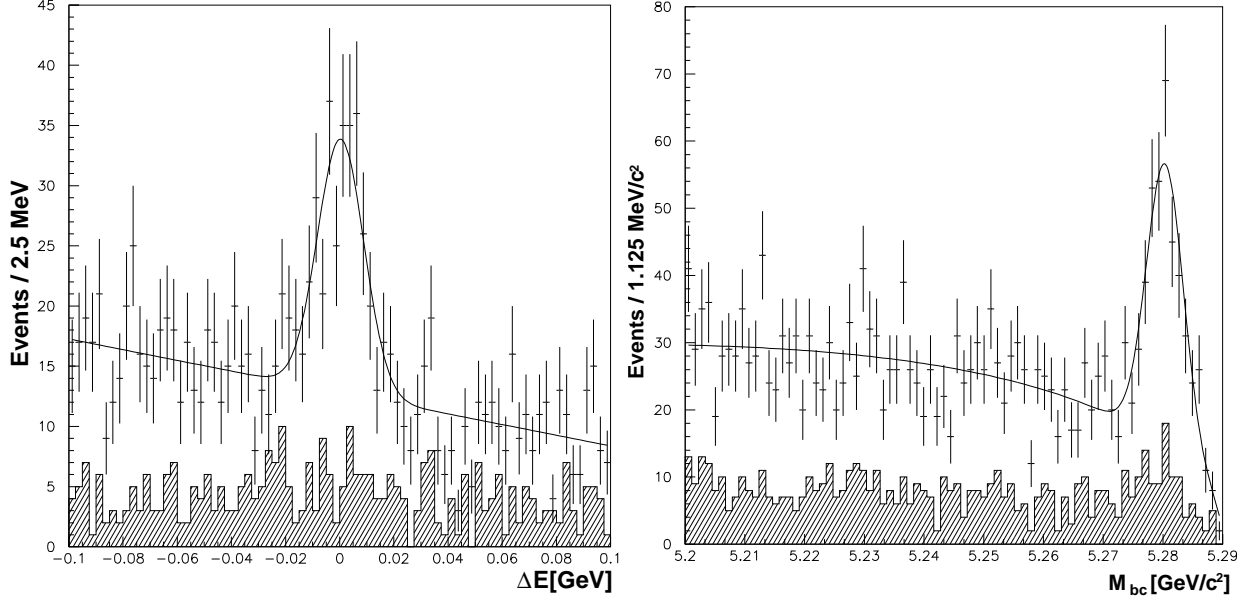


FIG. 2: ΔE (left) and M_{bc} (right) distribution for the D_s sideband. The hatched histogram is the contribution of events reconstructed in the $D_s^- \rightarrow \phi\pi^-$ and $D_s^- \rightarrow K_s^0 K^-$ decay modes where no significant peaks are observed. The full line is the result of the fit used to determine the $\bar{B}^0 \rightarrow D^+ K^{*0} K^-$ contribution.

also includes a small fraction of D_s signal that populates the D_s sideband. This contribution was evaluated using the simulated sample and subtracted from the fitted number of events in the peak.

Taking into account the contributions from non-resonant $D_s^- \rightarrow K^+ K^- \pi^-$ decays (evaluated using MC simulated events) and from $\bar{B}^0 \rightarrow D^+ K^{*0} K^-$ decays, we determine the number of signal $\bar{B}^0 \rightarrow D_s^- D^+$ in the sample to be [17] $N_{D_s D} = (1 - r_{KK\pi} - r_{DK^*K})N_{\text{data}} = 1287 \pm 40$, where the error is statistical only.

$\bar{B}^0 \rightarrow D_s^+ D_s^-$ decays

The selection optimized for the reconstruction of D_s^- decays in the $\bar{B}^0 \rightarrow D_s^- D^+$ events was also used to search for $\bar{B}^0 \rightarrow D_s^+ D_s^-$ decays. In this case two D_s meson candidates were searched for in each event using the decay modes listed above. The M_{bc} and ΔE variables are then calculated.

An additional source of background in this decay channel is a cross-feed from $\bar{B}^0 \rightarrow D_s^- D^+$ decays, where the D^+ decays into a $K^- \pi^+ \pi^+$ or $\bar{K}^0 \pi^+$ final state, and one of the pions is misidentified as a kaon. Although these events are shifted from zero in the ΔE distribution, they make observation of a small possible signal difficult. In order to reduce this contribution, we calculated for each candidate $D_s^\pm \rightarrow K^+ K^- \pi^\pm$ or $K_s^0 K^\pm$ decay the invariant mass of the final states particles with the π^\pm mass substituted for the K^\pm mass. If the invariant mass was within 20 MeV/ c^2 of the nominal D^\pm mass the event was rejected. The MC efficiencies for the reconstruction of $\bar{B}^0 \rightarrow D_s^+ D_s^-$ events for different combinations of D_s^\pm decay modes are determined and used for calculation of the overall efficiency $\epsilon(D_s D_s) =$

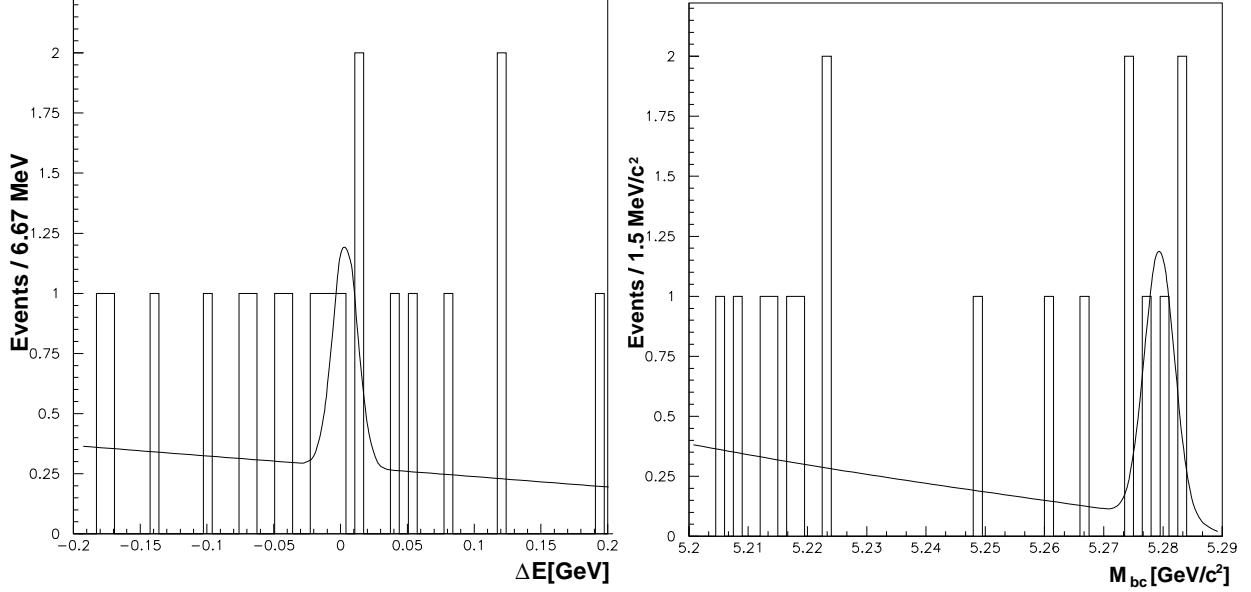


FIG. 3: ΔE (left) and M_{bc} (right) distributions for the $\bar{B}^0 \rightarrow D_s^+ D_s^-$ decay mode.

$\sum_{i,j=1,3} \epsilon_{i,j} \mathcal{B}(D_{si}) \mathcal{B}(D_{sj}) = (1.63 \pm 0.39) \times 10^{-4}$. Again, the main uncertainty ($\pm 23.1\%$) arises from the uncertainty in the intermediate branching fractions [6, 15]. The same efficiency expressed in terms of $\mathcal{B}(D_s^+ \rightarrow \phi \pi^+)$ reads $\epsilon(D_s D_s) = (0.383 \pm 0.040) \cdot (\mathcal{B}(D_s^+ \rightarrow \phi \pi^+) \mathcal{B}(\phi \rightarrow K^+ K^-))^2$.

The distributions of ΔE and M_{bc} for $\bar{B}^0 \rightarrow D_s^+ D_s^-$ candidates are shown in Fig. 3. No significant signal is observed. The distributions are fitted using a parameterization of the $D_s^- D^+$ mode. However, the signal ΔE distribution is described by a single Gaussian and the position and the width of the signal are fixed to the values obtained from the MC and rescaled by corresponding factors evaluated for the $D_s^- D^+$ mode. A binned likelihood fit gives $N_{D_s D_s} = 3.2 \pm 2.3$ signal events in the ΔE distribution, where the error reflects the statistical uncertainty. The corresponding value for a fit to the M_{bc} distribution is 4.7 ± 2.6 events.

The sidebands were used to check for a possible peaking background. No structure is observed in any of the M_{bc} - ΔE distributions for events in the D_s mass sidebands (see Fig. 4). If the D mass region is included in the D_s sideband, we observe a clear contribution from $\bar{B}^0 \rightarrow D_s^- D^+$ as expected.

Results

The number of signal $\bar{B}^0 \rightarrow D_s^- D^+$ events $N_{D_s D}$ is converted into a branching fraction using the efficiency $\epsilon(D_s D)$ and the number of $B\bar{B}$ events (assuming equal production of $B^0 \bar{B}^0$ and $B^+ B^-$ pairs): $\mathcal{B}(\bar{B}^0 \rightarrow D_s^- D^+) = (7.42 \pm 0.23) \times 10^{-3}$.

In addition to the above statistical error, we considered several sources of systematic uncertainty as listed in Table I. The largest contribution arises due to imprecise knowledge of the intermediate branching fractions of D_s and D mesons ($\pm 13.9\%$). We assigned a 1% relative error for each of the charged tracks used in the reconstructed final states due to

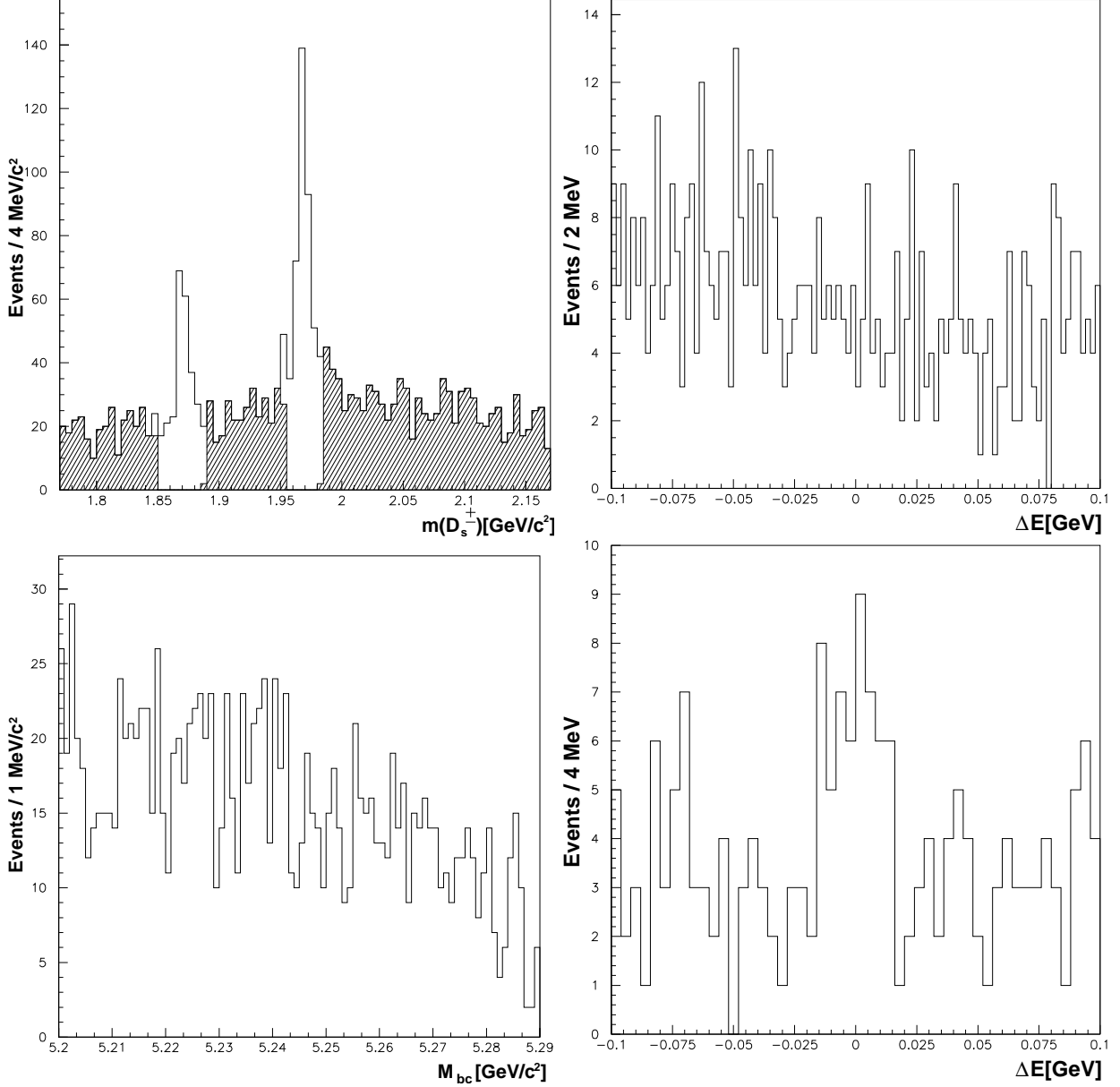


FIG. 4: Invariant mass of D_s^\pm candidates with hatched sidebands (upper left). ΔE (upper right) and M_{bc} (lower left) distribution for events with both D_s masses in the sideband. ΔE (lower right) for D_s^\pm signal candidate combined with a D_s^\mp from a sideband which includes the D^\mp mass region.

the uncertainty in tracking efficiency. The particle identification efficiency has a relative uncertainty of 2.5% per charged kaon and 2.0% per charged pion. An additional 1.4% uncertainty is due to the limited statistics of the MC sample used to estimate the efficiency. The fraction of true signal events in the sample ($1 - r_{KK\pi} - r_{DK^*K}$) is known to an accuracy of $\pm 2.2\%$. Systematics arising from the description of the ΔE distribution are evaluated by comparing the known number of reconstructed $\bar{B}^0 \rightarrow D_s^- D^+$ events in the simulated sample with the fitted yield and is found to be 2.2%. Finally, the uncertainty on the number of $B\bar{B}$ events (1.1%) is taken into account. The sum in quadrature of the individual contributions

TABLE I: Sources of systematic uncertainty in $\mathcal{B}(\overline{B}^0 \rightarrow D_s^- D^+)$ and $\mathcal{B}(\overline{B}^0 \rightarrow D_s^+ D_s^-)$ measurements.

$\overline{B}^0 \rightarrow D_s^- D^+$		$\overline{B}^0 \rightarrow D_s^+ D_s^-$	
Source	Rel. syst. error [%]	Source	Rel. syst. error [%]
D_s and D \mathcal{B} 's	13.9	D_s \mathcal{B} 's	23.1
Tracking	6.0	Tracking	6.0
Kaon ident.	7.1	Kaon ident.	8.5
Pion ident.	6.4	Pion ident.	5.2
MC statistics	1.4	MC statistics	5.3
$r_{KK\pi}, r_{DK^*K}$	2.2	Fixed parameters	4.1
Fitting model	2.2	Fitting model	9.5
$N(B\overline{B})$	1.1	$N(B\overline{B})$	1.1
Total	18.3	Total	28.4

gives a systematic error of 18.3%. The measured branching fraction is thus

$$\mathcal{B}(\overline{B}^0 \rightarrow D_s^- D^+) = (7.42 \pm 0.23(\text{stat.}) \pm 1.36(\text{syst.})) \times 10^{-3}. \quad (1)$$

The same result can be expressed by separating the largest source of systematic uncertainty, $\mathcal{B}(D_s^- \rightarrow \phi\pi^-) \mathcal{B}(\phi \rightarrow K^+K^-)$, in order to allow the result to be rescaled to future improved measurements of this quantity. In this case, the error arising from intermediate \mathcal{B} 's reduces to 7.7% [18] and $\mathcal{B}(\overline{B}^0 \rightarrow D_s^- D^+) \cdot \mathcal{B}(D_s^- \rightarrow \phi\pi^-) \mathcal{B}(\phi \rightarrow K^+K^-) = [1.47 \pm 0.05(\text{stat.}) \pm 0.21(\text{syst.})] \times 10^{-4}$.

We observe no statistically significant signal in the $\overline{B}^0 \rightarrow D_s^+ D_s^-$ decay mode. From the fitted number of events $N_{D_s D_s}$ we derive $\mathcal{B}(\overline{B}^0 \rightarrow D_s^+ D_s^-) = (7.1 \pm 5.1) \times 10^{-5}$, with a statistical error only. Applying the Feldman-Cousins [19] upper limit procedure to this value gives $\mathcal{B}(\overline{B}^0 \rightarrow D_s^+ D_s^-) \leq 1.6 \times 10^{-4}$ at 90% C.L.

Evaluation of systematic errors follows closely the treatment of the $\overline{B}^0 \rightarrow D_s^- D^+$ decay mode. Individual sources contributing to $\mathcal{B}(\overline{B}^0 \rightarrow D_s^+ D_s^-)$ are listed in Table I. The error arising from fitting was estimated by comparing the fitted and true number of simulated signal events. Additional uncertainty arises due to the use of a fixed width and position of the Gaussian function in the fit. The fit was repeated with parameters changed by one standard deviation; this resulted in a 4.1% change in \mathcal{B} . The overall systematic error is found to be 28.4%. We inflate the upper limit by this amount to obtain

$$\mathcal{B}(\overline{B}^0 \rightarrow D_s^+ D_s^-) \leq 2.0 \times 10^{-4} \quad \text{at 90\% C.L.} \quad (2)$$

Conclusions

We have measured the branching fraction for $\overline{B}^0 \rightarrow D_s^- D^+$ decays. The measured value is $\mathcal{B}(\overline{B}^0 \rightarrow D_s^- D^+) = [7.42 \pm 0.23(\text{stat.}) \pm 1.36(\text{syst.})] \times 10^{-3}$, which represents a large improvement in accuracy as compared to previous measurements.

This branching fraction can be used to obtain a value for the CKM matrix element $|V_{ub}|$ following [5]. Using $\mathcal{B}(\overline{B}^0 \rightarrow D_s^- \pi^+)$ from [1], we obtain $|V_{ub}/V_{cb}| = (7.4 \pm 1.2) \times 10^{-2}$. The

error includes experimental uncertainties on the measured branching fractions (the largest individual contribution is due to the statistical error on $\mathcal{B}(\overline{B}^0 \rightarrow D_s^- \pi^+)$ measurement, while the uncertainty on the $\mathcal{B}(D_s^+ \rightarrow \phi \pi^+)$ cancels in the ratio), as well as the uncertainty of the theoretical prediction. This result is in agreement with measurements from semileptonic decays [6].

For $\overline{B}^0 \rightarrow D_s^+ D_s^-$ decays we find no statistically significant signal. We set an upper limit of $\mathcal{B}(\overline{B}^0 \rightarrow D_s^+ D_s^-) \leq 2.0 \times 10^{-4}$ at 90% C.L. This result is the first limit on this decay mode and is below the prediction of [3].

We thank the KEKB group for the excellent operation of the accelerator, the KEK cryogenics group for the efficient operation of the solenoid, and the KEK computer group and the National Institute of Informatics for valuable computing and Super-SINET network support. We acknowledge support from the Ministry of Education, Culture, Sports, Science, and Technology of Japan and the Japan Society for the Promotion of Science; the Australian Research Council and the Australian Department of Education, Science and Training; the National Science Foundation of China under contract No. 10175071; the Department of Science and Technology of India; the BK21 program of the Ministry of Education of Korea and the CHEP SRC program of the Korea Science and Engineering Foundation; the Polish State Committee for Scientific Research under contract No. 2P03B 01324; the Ministry of Science and Technology of the Russian Federation; the Ministry of Higher Education, Science and Technology of the Republic of Slovenia; the Swiss National Science Foundation; the National Science Council and the Ministry of Education of Taiwan; and the U.S. Department of Energy.

-
- [1] K. Abe *et al.*, Belle Collaboration, hep-ex/0408109.
 - [2] A. Drutskoy *et al.*, Belle Collaboration, Phys. Rev. Lett. **94**, 061802 (2005).
 - [3] J. O. Eeg, S. Fajfer, A. Prapotnik, hep-ph/0501031.
 - [4] M. Kobayashi and T. Maskawa, Prog. Theor. Phys. **49**, 652 (1973);
N. Cabibbo, Phys. Rev. Lett. **10**, 531 (1963).
 - [5] C. S. Kim *et al.*, Phys. Rev. **D63**, 094506 (2001).
 - [6] S. Eidelman *et al.*, Phys. Lett. **B592**, 1 (2004).
 - [7] A. Abashian *et al.*, Belle Collaboration, Nucl. Instr. Meth. **A479**, 117 (2002).
 - [8] S. Kurokawa and E. Kikutani, Nucl. Instr. Meth. **A499**, 1 (2003), and other papers included in this Volume.
 - [9] Events are generated with the CLEO QQ generator (see <http://www.lns.cornell.edu/public/CLEO/soft/qq>); the detector response is simulated with GEANT, R. Brun *et al.*, GEANT 3.21, CERN Report DD/EE/84-1, 1984.
 - [10] Y. Ushiroda *et al.*, Nucl. Instr. Meth. **A511**, 6 (2003).
 - [11] K. Abe *et al.*, Belle Collaboration, Phys. Rev. **D66**, 032007 (2002).
 - [12] Inclusion of charge conjugate states is implicit throughout this report.
 - [13] G. C. Fox, S. Wolfram, Phys. Rev. Lett. **41**, 1581 (1978).
 - [14] H. Albrecht *et al.*, Argus Collaboration, Phys. Lett. **B241**, 278 (1990).
 - [15] B. Aubert *et al.*, BaBar Collaboration, hep-ex/0502041.
 - [16] A. Drutskoy *et al.*, Belle Collaboration, Phys. Lett. **B542**, 171 (2002).
 - [17] Since the simulated sample does not include the $\overline{B}^0 \rightarrow D^+ K^{*0} K^-$ contribution, an exact

- expression for $N_{D_s D}$ would include a correction of $r_{KK\pi} \cdot r_{DK^*K}$, which is negligible.
- [18] Uncertainties in $\mathcal{B}(D_s^- \rightarrow K^{*0}K^-)$ and $\mathcal{B}(D_s^- \rightarrow K_S^0 K^-)$ measured relative to the $\mathcal{B}(D_s^- \rightarrow \phi\pi^-)$ [6].
- [19] G. J. Feldman, R. D. Cousins, Phys. Rev. **D57**, 3873 (1998).